JOURNAL OF OPTOELECTRONICS AND ADVANCED MATERIALS Vol. 15, No. 7-8, July - August 2013, p. 703 - 706

Sol-gel synthesis and optical properties of ZnO powder

A. MATEI[a,b*], L. DUMITRESCU[b], I. CERNICA[a], V. SCHIOPU[a], A. DINESCU[a], M. DANILA[a],
I. MIHALACHE[a], I. MANCIULEA[b]
[a]*National Institute for Research and Development in Microtehnologies Bucharest, Erou Iancu Nicolae Street, 126A, 077190, Romania*
[b]*Transilvania University of Brasov, B-dul Eroilor 29, 500036, Romania*

Zinc oxide (ZnO) powders with various morphologies present unique properties and can be used in technological applications, such as optics, electronics, ceramics, coatings, biology and many other areas. This paper presents the synthesis and characterization of ZnO powder by sol-gel method using different types of solvents. After drying process, the samples were annealed at 500°C to obtain nanocrystalline ZnO powders. The morphology, composition and optical properties of the obtained powders were investigated by using scanning electronic microscopy (SEM), X-ray diffractometry (XRD), Fourier transformed infrared spectroscopy (FTIR), energy dispersive X-ray spectroscopy (EDX) and photoluminescence (PL). The characterization reveals that the ZnO samples consist of a mixture of nanoparticles and nanorods with different size and shape. The X-ray diffraction also determined the ZnO nanoparticles have a high purity, wurtzite crystalline structure. Based on these results, the properties of the ZnO samples were correlated with their morphology and structure.

(Received March 25, 2013; accepted July 11, 2013)

Keywords: Zinc oxide, Nanopowder, Sol-gel method, Characterization

1. Introduction

Zinc oxide (ZnO) powder has been widely studied and received a considerable attention due to its special properties and wide range of technologically applications. In particular, ZnO is an interesting material with a wide band gap (3.37eV) and large binding energy (60meV), used for light emitting diodes, varistors, solar cell, pigments, sensors, dielectrics, transparent UV-protection films, antibacterial agents, piezoelectric devices, photocatalysis and so on [1, 2].

Zinc oxide is a nanostructured material because it can exists in different morphologies, like nanoparticles, nanorods, nanowires, nanotubes or thin films and can be synthesized by various chemical techniques including hydrothermal synthesis [3], precipitation [4], spray pyrolysis [5] and sol-gel method [6-7].

It is known, that the crystallite size and the morphology of the ZnO nanoparticles depends of the synthesis method. Among chemical method, the sol-gel process is one of the most interesting methods because of the following advantages: good homogeneity, ease of composition control, low processing temperature, repeatability, simplicity, low equipment cost and good optical properties [8, 9].

Also, to investigate the details of chemical process, some factors such as reaction time, synthesis temperature, surfactants, polymers, solvents, ultrasonic pretreatment of the solution mixture, must be considered, in order to obtain final products [10].

In addition, by using the sol-gel process, nanoparticles with various morphologies and size by changing the solvents can be obtained [11-12].

In this paper, we report on the influence of solvents on the synthesis and characterization of zinc oxide nanoparticles by sol-gel method and their characterization by using scanning electronic microscopy (SEM), X-ray diffractometry (XRD), Fourier transformed infrared spectroscopy (FTIR), energy dispersive X-ray spectroscopy (EDAX) and photoluminescence (PL).

2. Experimental

2.1. Materials

Zinc acetate dihydrate [$Zn(CH_3CO_2)_2$ $2H_2O$], glacial acetic acid [CH_3COOH], polyethylene glycol ($H(OCH_2CH_2)nOH$, PEG), ethanol (C_2H_5OH), deionized water, ammonia solution 25% (NH_4OH) from CHIMOPAR were used. All chemicals were used as received, without further purification.

2.2. Synthesis of ZnO nanoparticles

In our experiments we used zinc acetate dihydrate [$Zn(CH_3CO_2)_2$ $2H_2O$], acetic acid (CH_3COOH), polyethylene glycol ($H(OCH_2CH_2)nOH$, PEG), ethanol (C_2H_5OH) and deionized water as starting materials and solvents.

Fig. 1 shows a flowchart of sol-gel method for preparation ZnO nanoparticles.

According to the scheme, an amount of [$Zn(CH_3CO_2)_2$ $2H_2O$] was dissolved into certain solvent of ethanol, or water, respectively.

Various amounts of acetic acid (CH_3COOH) or/and surfactants ($H(OCH_2CH_2)nOH$, PEG) were dissolved in 50ml deionized water under vigorous stirring for 1h.

Then, acetic acid (CH_3COOH) was dropped into both (1 and 2) solutions of zinc acetate under constant stirring. After that, the polyethylene glycol ($H(OCH_2CH_2)nOH$, PEG) surfactant was added into the solution (2) of ethanol, and did not added into the aqueous solution (1). The pH of both solutions was adjusted at 8 with ammonia solution (alkaline condition).

The resulting white gels were stirred for 1h at 80°C and were further dried at 200°C for 2h and calcined at the temperature over 500°C.

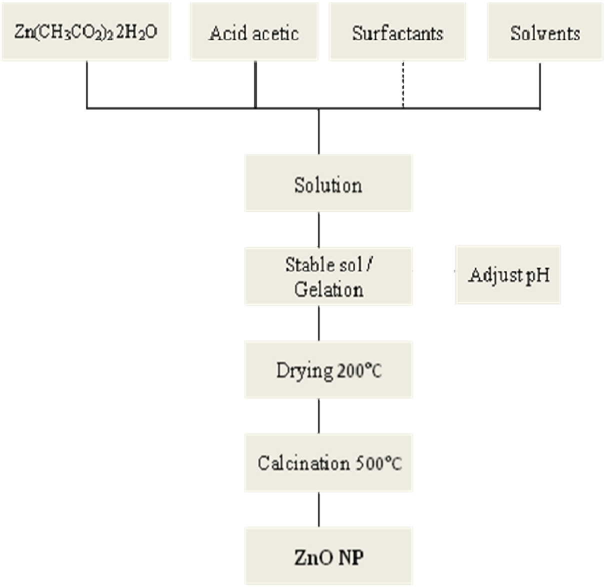

Fig. 1. Flowchart of sol-gel method for preparation ZnO nanoparticles.

2.3. Characterization of ZnO nanoparticles

The morphology and components of the ZnO samples were characterized using Nova NanoSEM 630, a Field Emission Scanning Electron Microscope (FE-SEM) (FEI Company, USA) and energy dispersive X-ray spectrometer (EDX).

Phase identification, crystallite size and lattice parameter were analyzed by X-ray diffractometry (XRD), using a Rigaku Smartlab thin film 9kW rotating anode equipped with an in-plane arm θ-2θ angular scanning configuration with a Cu X-ray tube, a multilayer mirror (parallel beam, X-ray Kα wavelength λKα= 1. 540593Å).

The bonding configuration of powders was analysed by Fourier Transform Infrared (FTIR) spectrometry at room temperature using a Bruker Tensor 27 spectrometer, in the range of 4000 - 400cm^{-1} by averaging 64 scans with a resolution of 4 cm^{-1}. The samples were mixed with KBr and compressed into pellets with a hydraulic press at pressure of 10 tons for 5 min.

Photoluminiscence spectra were measured at the room temperature by fluorescence spectrometer (FLSP 920).

3. Results

3.1. Morphological analysis

SEM images of ZnO samples obtained by using various solvents are shown in Fig. 2 (a) and Fig. 2(b).

The SEM image of sample obtained in ethanol solution (Fig. 2(a), shows a mixture of particles with sizes ranging from 20-100nm and rods with diameters of 20-50 nm and 80-150 nm in length.

The ZnO powder samples obtained in aqueous medium have particles mostly spherical in shape, ranging from 20 to 80 nm, and a slightly tendency to agglomeration, as can be seen in SEM imagine (Fig. 2(b). It also was observed that the particles are bigger in size compared to those obtained in ethanol solution.

It seems that the solvent is a key factor for obtaining ZnO nanopowders of high quality.

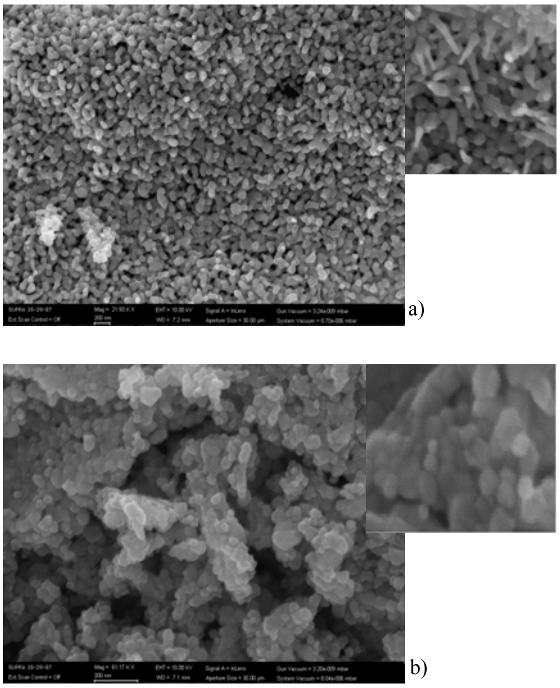

Fig. 2. SEM images of ZnO powders using various solvents (a) ethanol, (b) water.

3.2. Elemental analysis by EDX

The chemical composition of the ZnO samples was investigated by using EDX. The results of EDX analysis (see

Fig. 3(a) and Fig. 3(b)) established that powders are formatted only from zinc and oxygen, no other peak of another element wasn't found in the spectrum, assessing the purity of the samples.

In both samples, the atomic ratio of zinc and oxygen were 51.53 : 48.47 and 55.84 : 44.16, which is nearly 1 : 1 atomic percentage, confirming the formation of stoichiometric ZnO.

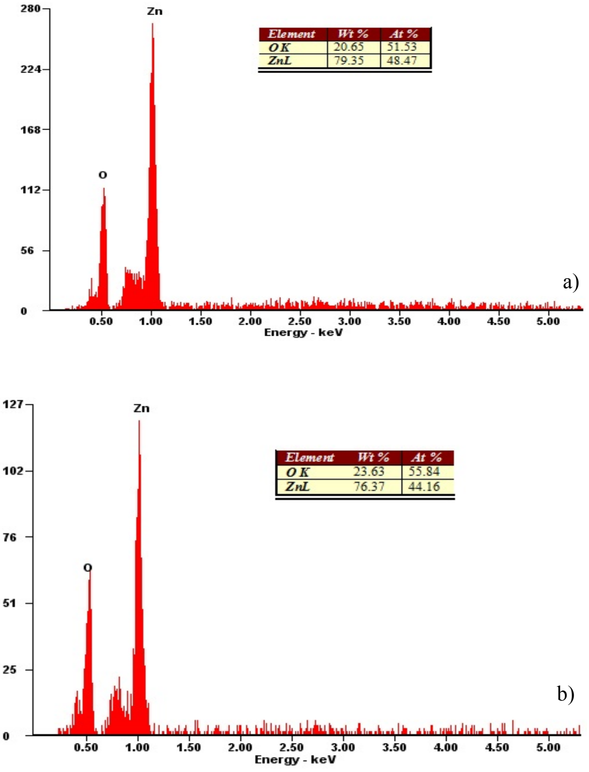

Fig. 3. EDX of ZnO powders obtained by using various solvents (a) ethanol, (b) water.

3.3. X-Ray diffraction analysis

The XRD patterns of the synthesized ZnO samples using different solvents, like ethanol and water are presented in Fig. 4(a) and Fig. 4(b). For both samples, the diffraction peaks were indexed to hexagonal phase ZnO with lattice constants a=b= 3.25A and c =5.20A.

The XRD pattern of ZnO sample (Fig. 4(a)) indicates no peaks from another phase, belonging to precursor compounds or impurities, certifying the high purity of ZnO.

In Fig. 4(b) the XRD pattern presents some impurities from unreacted zinc acetate.

The average crystallite sizes of the ZnO samples were calculated using Scherrer's equation. The particles size varied from 20nm (pure ZnO) to 35nm (ZnO with impurities), indicating that the type of solvents influence the crystallite size.

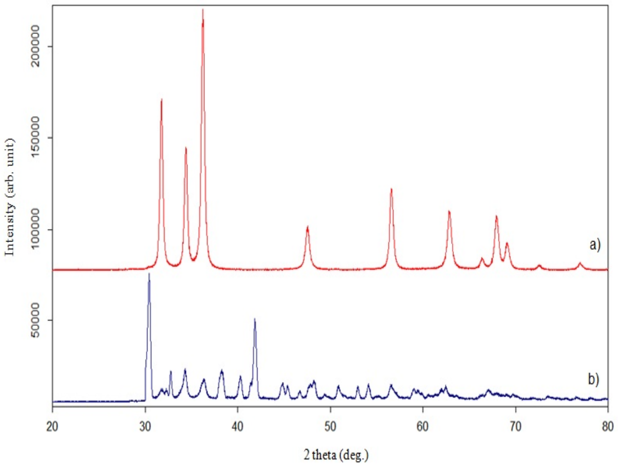

Fig. 4. XRD of ZnO powders using various solvents (a) ethanol, (b) water.

3.4. FTIR analysis

FTIR is the most useful technique used to obtain information about the chemical bonding and identification the characteristic groups on the surface of ZnO samples.

The FTIR spectra for ZnO samples presented in Fig. 5(a) and Fig. 5(b) show the characteristic peaks at 432, 441, 490 and 502cm^{-1}, which can be assigned to the stretching vibration mode of Zn-O.

The bands located in the range 4000 – 600cm^{-1} are associated to organic groups and to the OH stretching mode, indicating the presence of small amount of water adsorbed on the surface of ZnO nanoparticles.

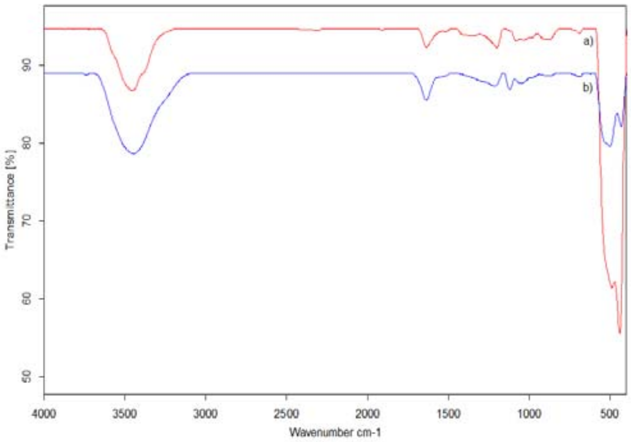

Fig. 5. FTIR spectra of ZnO powders using various solvents (a) ethanol, (b) water.

According to the literature, the shape and the position of the absorption bands can be correlated with both the crystal structure and chemical composition and with the size and morphology of the particles [13].

3.5. Photoluminescence analysis

For the investigation of the optical properties of ZnO nanopowders obtained in different solvents, photoluminescence (PL) spectra were measured at the room temperature with an excitation wavelength of 350nm.

The PL spectrum of ZnO powder obtained from ethanol solution (Fig. 5(a)) shows an intense photoluminescence emission with a single peak at 397nm.

The PL spectrum of ZnO powder obtained from aqueous solution (Fig. 5(b)) exhibits two emission peaks, one is centred at around 396nm corresponding to the electron transition from a shallow donor level of neutral zinc interstitials to the top level of the valence band. A weak peak is also observed at around 509 nm, which derived from the electron transition from the level of the ionized oxygen vacancies to the conduct band.

Over the years, several authors have investigated the photoluminescent properties of ZnO nanostructures. In general, the band edge emission at ~396 nm is attributed to the recombination of excitons. Usually, the visible emission from ZnO is allocated to different intrinsic defects such as oxygen vacancies (V_o), zinc vacancies (V_{Zn}), oxygen interstitial (O_i), zinc interstitial Z_{ni} and oxygen antisites O_{Zn} [14, 15].

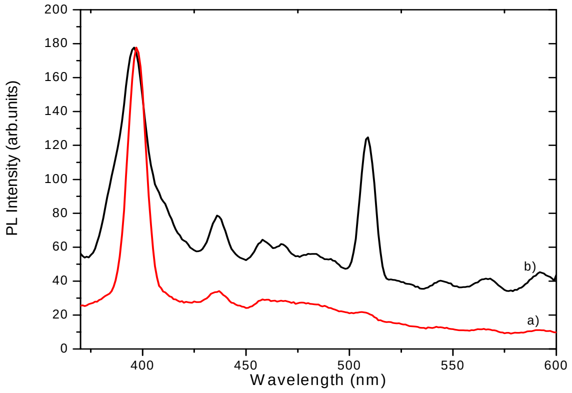

Fig. 5. PL spectra of ZnO powders using various solvents (a) ethanol, (b) water.

It can be seen that the photoluminescence spectra of ZnO powders obtained in various solvent have a same shape and a slightly intensity difference due to the wide distribution of the particles size. The intensity of peaks of the ZnO powder obtained using ethanol as solvent is much lower compared to the absorption peak of ZnO sample in aqueous solution.

4. Conclusions

ZnO nanopowders were obtained by sol-gel method using zinc acetate as source for zinc and aqueous and organic solvents in similar conditions.

The SEM analysis confirms XRD analysis and shows the particles size in the range of 20-80nm for ZnO powder using water and ethanol solvent, respectively. Meantime, the SEM clearly shows microstructural homogeneities and different morphology (nanorods and nanoparticles of various sizes) in various solvents, indicating that the choise of solvents is a important factor for synthesis of ZnO nanopowder. From EDX, it is suggested that the powders chemical composition is ZnO.

The XRD patterns confirms the hexagonal structure of ZnO nanoparticles, but with different crystallite size.

The photoluminescent results confirmed by XRD and PL showing that sample using ethanol as presents a better crystallinity than that of sample using water.

The FTIR spectrum of ZnO powder annealed at 500°C exhibits the bands in the range 400-500cm^{-1}, which are characteristic to the vibrational mode of Zn-O.

The optical properties of ZnO samples were analyzed by photoluminescence spectra and present in both cases a strong emission band characteristic to ZnO.

References

[1] A. Azam, F. Ahmed, N. Arshi, M. Chaman, A. H. Naqvi, Journal of Alloys and Compounds **496**, 399 (2010).
[2] Z. Fan, J. G. Lu, Journal of Nanoscience and Nanotechnology **5**(10), 1561 (2005).
[3] P. M. Aneesh, K. A. Vanaja, M. K. Jayaraj, , Nanophotonic Materials IV, Proc. SPIE **6639**, 66390J-1-9 (2007).
[4] C. Chen, B. Yu, P. Liu, J. F. Liu, L. Wang, Journal of Ceramic Processing Research., **12**(4), 420 (2011).
[5] G. H. Reza, S. Mahboobeh, S. Mohammad Ali, Iranian Journal of Chemistry & Chemical Engineering, **13**(1), (2011).
[6] B. Sudheer Kumar, International Journal of Engineering Research & Technology, **1**, (2012).
[7] Y. L. Zhang, Y. Yang, J. H. Zhao, R. Q. Tan, P. Cui, W. J. Song, Journal of Sol-Gel Science and Technology, **51**, 198 (2009).
[8] Y. Dimitriev, Y. Ivanova, R. Iordanova, Journal of the University of Chemical Technology and Metallurgy, **43**(2), 181 (2008).
[9] M. Raileanu, Revue Roumaine de Chimie, **51**(10), 941 (2006).
[10] M. Rezapour, N. Talebian, Materials Chemistry and Physics, **129**, 249 (2011).
[11] K. G. Kanade, B. B. Kale, R. C. Aiyer, B. K. Das, Materials Research Bulletin **41**, 590 (2006).
[12] B. Ranjan, M. Kailasnath, N. Kumar, P. Radhakrishnan, S. Achari, V. P. N. Nampoori, Transport and optical properties of nanomaterials: Proceedings of the ‘ International Conference-ICTOPON, AIP Conference Proceedings, **1147**, 287 2009.
[13] P. B. Khoza, M. J. Moloto, L. M. Sikhwivhilu, Journal of Nanotechnology, Article ID 195106, (2011).
[14] S. Talam, Rao S. Karumuri, N. Gunnam, IRSN Nanotechnology, Articles ID 372505, (2012).
[15] S. K. Mishra, R. K. Srivastava, S. G. Prakash, Journal of Alloys and Compounds, **539**, 1 (2012).

---

[*] Corresponding author: ileana.cernica@imt.ro